Supporting Information

Effects of 1,8-Diiodooctane on Domain Nanostructure and Charge Separation Dynamics in $PC_{71}BM$-Based Bulk Heterojunction Solar Cells

Sylvia J. Lou,[1] Nanjia Zhou,[2] Xugang Guo,[1,3] Robert P. H. Chang,[2*] Tobin J. Marks,[1,2]* Lin X. Chen[1,4]*

Affiliations

[1] *Department of Chemistry and the Argonne-Northwestern Solar Energy Research Center, Northwestern University, 2145 Sheridan Road, Evanston, Illinois 60208, United States*

[2] *Department of Materials Science and Engineering and the Argonne-Northwestern Solar Energy Research Center, Northwestern University, Evanston, Illinois 60208, United States*

[3] *Department of Materials Science and Engineering, South University of Science and Technology of China, No. 1088, Xueyuan Blvd, Shenzhen, Guangdong, 518055, China*

[4] *Chemical Sciences and Engineering Division, Argonne National Laboratory, Darien, Illinois 60439, United States*

Solar cell external quantum efficiency data

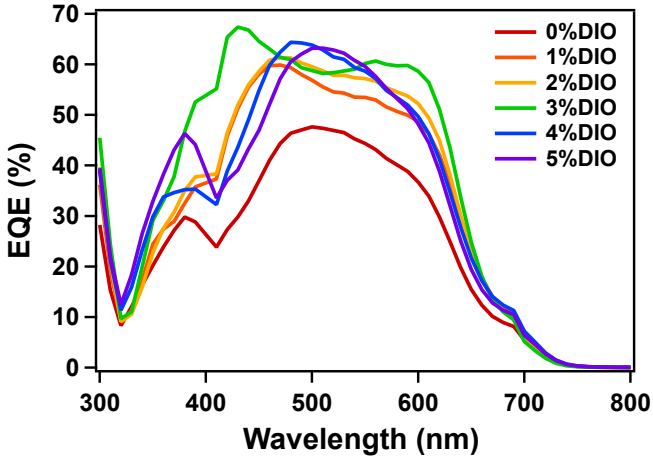

Figure S1. External quantum efficiencies of PBTIBDT:PCBM solar cells with 0-5 vol% DIO added to the active layer solution

Small angle x-ray scattering component fits forPBTIBDT+PCBM solutions with 0-5 vol% DIO

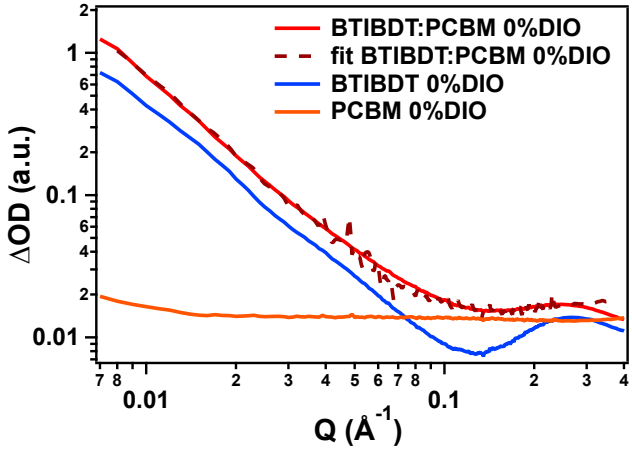

Figure S2. Representative fits of PBTIBDT+PCBM solution data with 0 vol% DIO

Table S1. Table of small angle x-ray scattering component fit percentages

[DIO] (vol%)	Percentage of each component	
	PCBM	PBTIBDT
0	6	94
1	5	95
2	5	95
3	3	97
4	4	96
5	4	96

GIWAXS data analysis procedures and 2D images

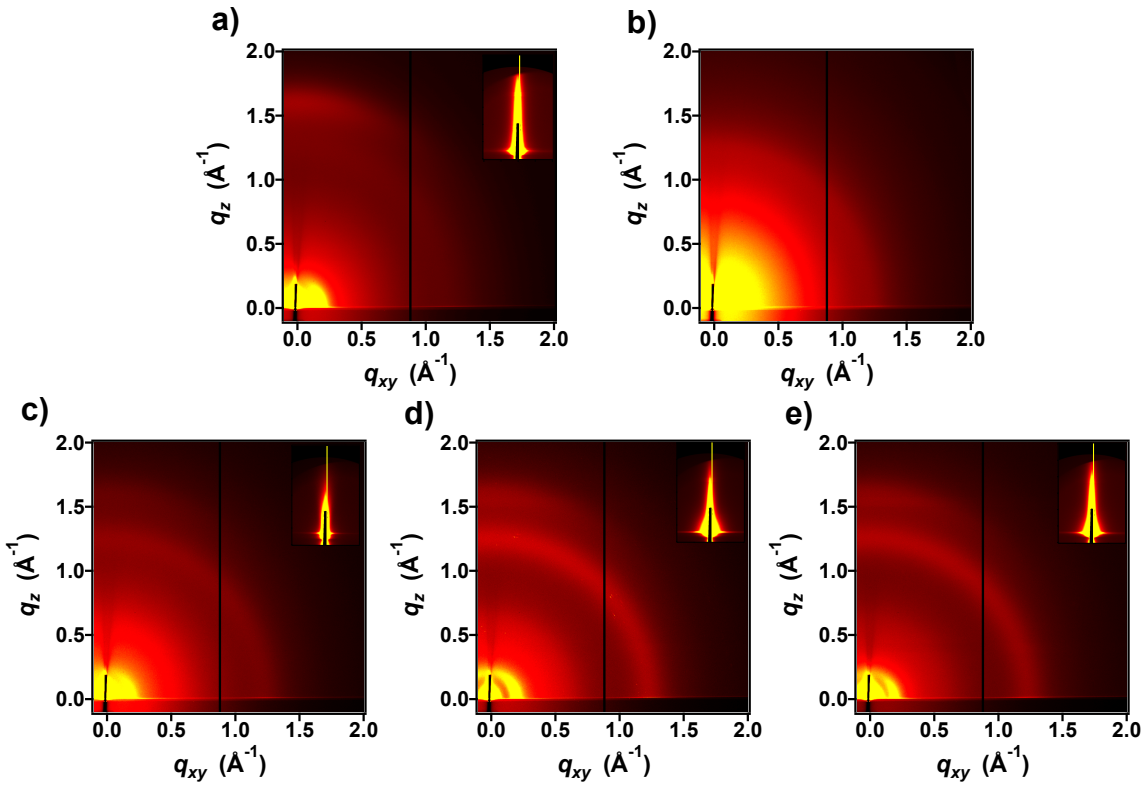

Figure S3. 2D GIWAXS images of neat films of a) PBTIBDT 0% DIO and b) PCBM and blend PBTIBDT:PCBM films with: c) 0 vol % DIO, d) 3 vol% DIO, e) 5vol% DIO.

Linecuts were taken parallel to the horizontal (q_{xy}) and vertical (q_z) axes to approximate the in-plane and out-of-plane structure of the polymer, respectively (Figure S4). The

background was subtracted by fitting the trace to an exponential decay and the peaks in the resulting trace were fit using 2-5 Gaussians, depending on the trace studied. One Gaussian was always used to fit the amorphous scattering feature from the substrate which has somewhat variable intensity in each scan.

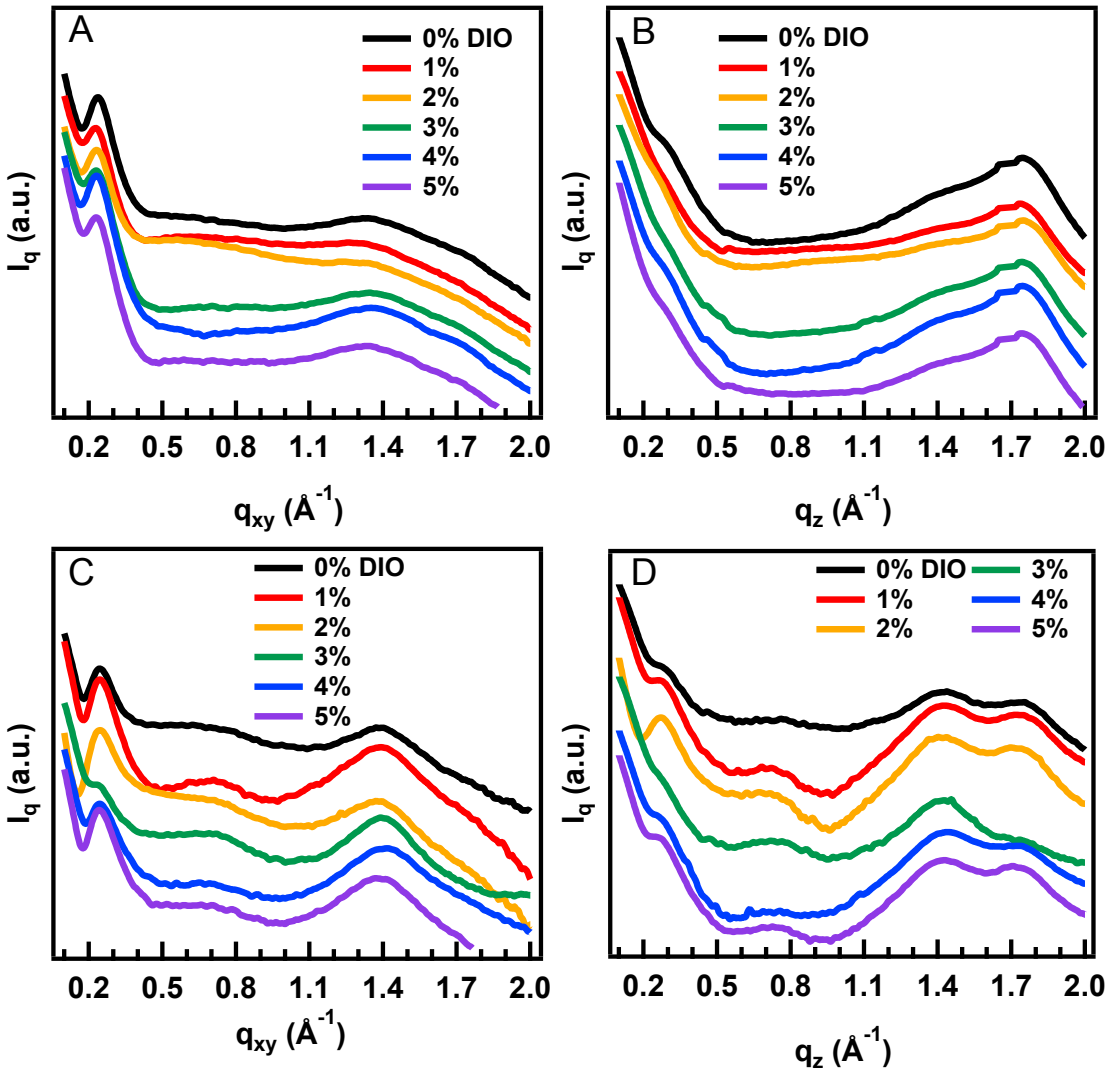

Figure S4. GIWAXS linecuts along the horizontal and vertical axes of the 2D images showing the crystal structure of A) neat PBTIBDT films with 0-5 vol % DIO in-plane and B) neat PBTIBDT films with 0-5 vol% DIO out of plane and C) PBTIBDT:PCBM films with 0-5 vol % DIO in-plane and PBTIBDT:PCBM films with 0-5vol % DIO out of plane.

Table S2. GIWAXS d-spacings of PBTIBDT and PCBM domains in neat and blend thin films as a function of vol% DIO.

DIO (vol %)	PBTIBDT lamellar (neat) (Å)	PBTIBDT π-π (neat) (Å)	PBTIBDT lamellar (blend) (Å)	PBTIBDT π-π (blend) (Å)	PCBM (neat) (Å)	PCBM (blend) (Å)
0	26.2	3.6	25.5	3.6	4.5	4.5
1	27.7	3.6	25.2	3.6	4.5	4.5
2	26.8	3.6	25.5	3.7	4.5	4.5
3	27.6	3.6	27.5	3.7	4.5	4.5
4	27.2	3.6	25.1	3.7	4.6	4.4
5	27.7	3.6	25.3	3.6	4.5	4.5

GISAXS data analysis and linecuts

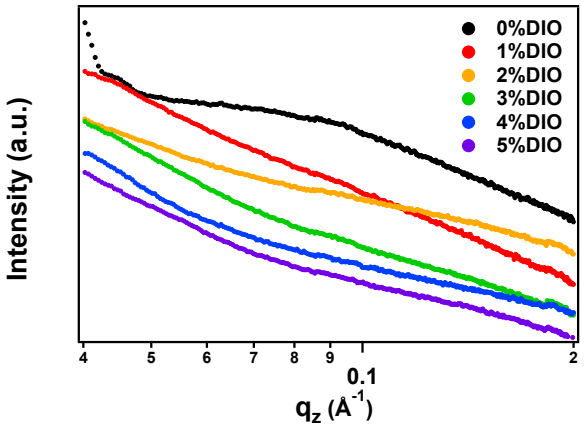

Figure S5. GISAXS linecuts of PBTIBDT:PCBM blend films with 0-5 vol% DIO describing the domain sizes out of plane.

Spectroelectrochemistry data for PBTIBDT cation signal determination in solutions and films

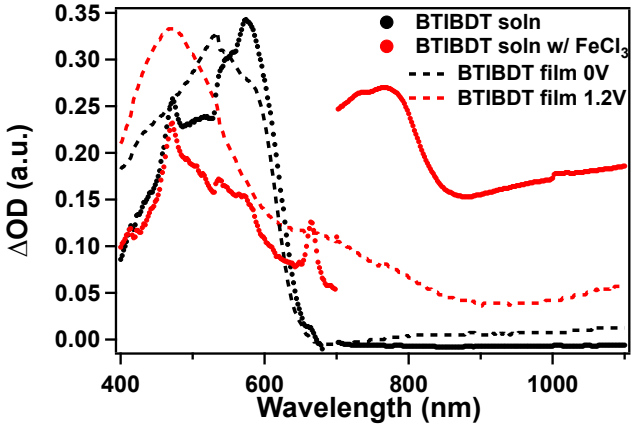

Figure S6: Spectroelectrochemisty of PBTIBDT solutions in *o*-dichlorobenzene and neat film showing cation signals at 750-800 nm with a broad feature extending from 1000 nm to longer wavelengths.

UV-Vis Absorption spectra for neat PBTIBDT films with 0-5 vol% DIO

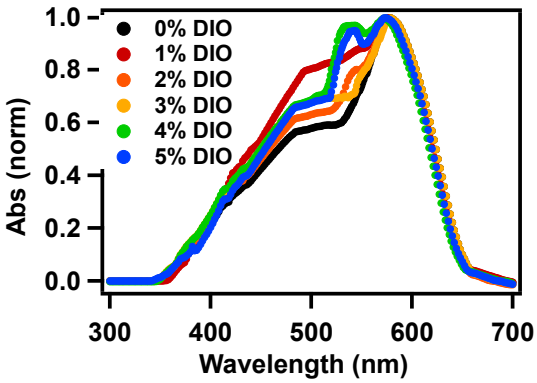

Figure S7: UV-Vis absorption spectra of neat PBTIBDT films with no DIO and 1-5 vol% DIO.

The absorption shows no change in onset absorption and minor shifts in the peak absorption, but an increase in the vibronic structure as DIO concentration is increased, suggesting increased crystallinity of the PBTIBDT regions as DIO concentration is increased.

Optical transient absorption within 3 ns delay time window, and fitting parameters for exciton absorption and ground state bleach

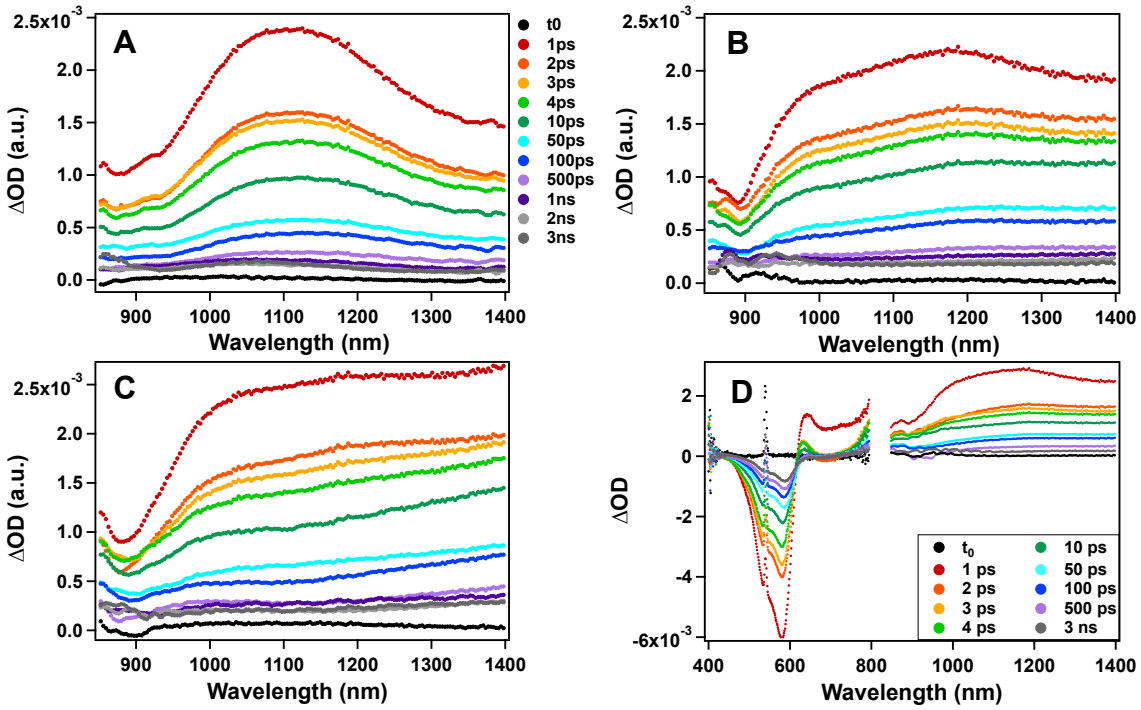

Figure S8: Time delays of A) neat PBTIBDT film with 0 vol% DIO and B) PBTIBDT:PCBM blend film with 0 vol% DIO and C) 5 vol% DIO and D) PBTIBDT:PCBM blend film with 3 vol% DIO illustrating the entire visible and near IR spectra.

Table S3: Exciton dynamics of PBTIBDT:PCBM blend films

[DIO] (vol %)	τ1 (ps)	τ2 (ps)	τ3 (ps)[a]	τ4 (ps)	A1 (%)	A2 (%)	A3 (%)	A4 (%)
0	0.48 (0.01)	4.3 (0.2)	82.8 (10.8)	>3000	57 (3)	15 (2)	22 (1)	6 (0)
1	0.56 (0.03)	5.0 (0.6)	63.8 (11.4)	>3000	64 (4)	8 (3)	22 (2)	6 (0)
2	0.76 (0.04)	4.8 (0.6)	84.3 (20.3)	>3000	59 (6)	11 (4)	22 (2)	8 (1)
3	0.61 (0.03)	5.2 (0.7)	62.6 (17.0)	>3000	61 (5)	10 (4)	21 (2)	8 (1)
4	0.29 (0.01)	3.4 (0.2)	86.7 (9.9)	>3000	70 (3)	12 (1)	13 (1)	4 (0)
5	0.54 (0.02)	4.3 (0.5)	53.6 (10.2)	>3000	64 (4)	10 (3)	20 (2)	6 (0)

[a] Attributed to CAT decay due to overlap of CAT and EX peaks.
Error in fit is noted in parentheses.

Table S4: Ground state bleach dynamics of PBTIBDT:PCBM blend films

[DIO] (vol %)	τ1 (ps)	τ2 (ps)	τ3 (ps)	τ4 (ps)	A1 (%)	A2 (%)	A3 (%)	A4 (%)
0	0.48 (0.01)	4.3 (0.2)	97 (8)	>3000	66 (1)	20 (1)	10 (0)	4 (0)
1	0.56 (0.03)	5.0 (0.6)	92 (10)	>3000	64 (1)	18 (1)	10 (1)	8 (0)
2	0.76 (0.04)	4.8 (0.6)	70 (10)	>3000	67 (2)	21 (2)	6 (1)	6 (0)
3	0.61 (0.03)	5.2 (0.7)	65 (11)	>3000	70 (1)	18 (1)	6 (1)	6 (0)
4	0.29 (0.01)	3.4 (0.2)	71 (5)	>3000	72 (1)	16 (0)	7 (0)	5 (0)
5	0.54 (0.02)	4.3 (0.5)	50 (8)	>3000	76 (1)	16 (1)	4 (1)	4 (0)

Error in fit is noted in parentheses.

Table S5: Dynamics of neat PBTIBDT films

		τ1 (ps)	τ2 (ps)	τ3 (ps)	A1 (%)	A2 (%)	A3 (%)	A4 (%)
0 vol % DIO	CS	0.39 (0.01)	NA	60.6 (10.0)	71 (9)	NA	26 (2)	3 (1)
	EX	0.39 (0.01)	4.3 (0.3)	NA	73 (4)	20 (2)	NA	7 (0)
	GSB	0.39 (0.01)	4.3 (0.3)	60.6 (10.0)	79 (1)	14 (0)	4 (0)	3 (0)
5 vol % DIO	CS	0.24 (0)	NA	68.2 (3.8)	69 (2)	NA	23 (1)	7 (0)
	EX	0.24 (0)	6.3 (0.4)	NA	70 (2)	26 (1)	NA	4 (0)

Error in fit is noted in parentheses.

Nanosecond transient absorption

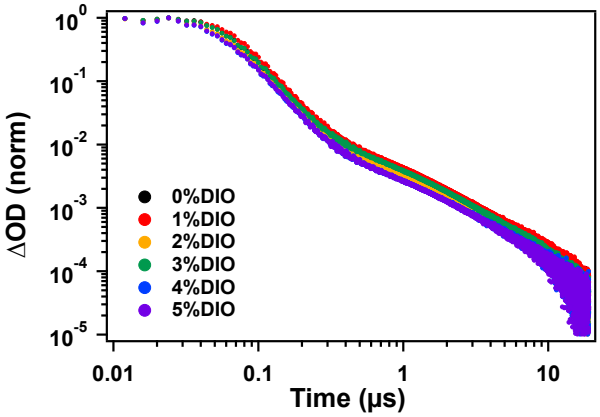

Figure S9. Decay of cation species at 1070 nm in PBTIBDT:PCBM films as a function of vol % DIO normalized at the highest intensity.